Methane combustion over Pd/Al-MCM-41catalysts: The effect of palladium precursors and the preparation route

Anis Gannouni*, Sonia Zribi, Rihem Dardouri, Mongia Saïd Zina

Université de Tunis El Manar, Faculté des Sciences de Tunis, Laboratoire de Chimie des Matériaux et Catalyse, Campus Universitaire, Tunis 2092, Tunisie.

(Received: 06 April 2016, accepted: 18 July 2016)

Abstract: The effect of palladium precursors and the preparation route on the catalytic performance of mesoporous materials Pd/Al-MCM-41 in methane oxidation was investigated in this work. The catalysts were prepared using both methods, namely hydrothermal method (DHT) and template ion exchange method (TIE), from three different palladium precursors $Pd(NH_3)_4Cl_2$, $PdCl_2(MeCN)_2$and $Pd(acac)_2$. All catalysts were characterized by a variety of physico-chemical techniques such as X-ray diffraction (XRD), N_2physisorption, H_2 chemisorption, temperature programmed desorption of H_2, diffuse reflectance UV–visible spectroscopy andelemental analysis by ICP, and then tested in methane combustion. According to the obtained results, the use of different palladium precursors and preparation routes play an important role on the catalytic properties of materials. The use of bis(acetonitrile)palladium (II) chloride as precursor by the TIE method seems to conduct to the best catalytic performance.This is in agreement with a better dispersion of PdO nanoparticles, thus optimizing the accessibility of reactants to the active sites in the mesoporous channels of Al-MCM-41.

Keywords: Al-MCM-41; Palladium; Template ion exchange; Hydrothermal; Methane.

INTRODUCTION

Over the past decade, the catalytic combustion of methane at low temperature has been a focus of great interest due to the increasing use of methane as an environmentally friendly fuel [1-4]. Numerous catalysts have been developed for methane C-H bond activation, the most efficient being supported noble metals such as Pd, Pt and Rh [5], transition metal oxides or bulk mixed-metal oxides [6]. The supported palladium catalysts are known to be extremely active for methane combustion reaction [7-11] which have been widely investigated in the literature [9-23]. Several studies have shown that PdO is the active phase for the catalytic combustion of methane [5, 13]. However, for the zeolite supported palladium catalysts, it has been demonstrated that the Pd / PdO pair is considered to be the active sites [24].

Furthermore, among the most investigated issues affecting the catalytic activity of these catalysts in methane combustion are the nature of active sites, Pd oxidation, metal–support interaction and active sites accessibility by reactants [5, 25-28]. Nevertheless, better dispersion of the metal may lead to greater stability of the supported PdO phases, which are less reducible according to RTP studies and therefore less active [22, 23]. The increase in catalytic activity of supported palladium catalysts was attributed to the ability to provide low interaction PdO particles with the support [22, 23].

Mesoporous silica such as MCM-41 and recently SBA-15 have also been used as a host support for the combustion of methane, due to their high surface area (≈1000 m^2 g^{-1}) which leads to high metal dispersion. [16-18, 28]. However, it is well known that, the incorporation of aluminium ions into the framework of mesoporous MCM-41 silica catalysts positively affects catalytic performance [17]. Indeed, it has been demonstrated that the supported Pd/Zeolite catalysts exhibit a

* Corresponding author, e-mail address : anis.gannouni@gmail.com

higher activity than Pd/Al_2O_3, mainly related to the highly dispersed PdO over zeolite supports [5]. These results are in good agreement with those reported by Wang et al. [17] who showed that the plasma treatment of the catalyst improves the dispersion of the supported PdO particles on Al-MCM-41, which are found to be more active. Simplicio et al. [29] have shown that the dispersion of metal particles depends on the nature of palladium precursor. Indeed, the use of palladium acetylacetonate as a precursor generated well-dispersed PdO particles on alumina. Recently, Zribi et al [7, 10] reported that the reactivity of Pd/ MCM-41 catalysts in methane combustion depends on the method of preparation, either via an in-situ sol-gel method or by grafting. The latter route of synthesis provides small, highly dispersed PdO nanoparticles leading to better activity, consistent with higher metal accessibility.

In addition, we have previously reported that Pd/Al-MCM-41 catalysts prepared by ion-exchange (TIE) method provide highly dispersed PdO particles in the mesoporous silica [28]. The use of this latter method with $Pd(NH_3)_4Cl_2$ as palladium precursor and the addition of Al^{3+} sites were likely acting as anchoring sites for the PdO particles favoring high metal dispersion of palladium which is counterbalanced by the loss of metal accessibility due to partial collapse of the support structure generating a partial encapsulation of metallic species.

Thereby the present work aims the characterization and reactivity of the Pd catalysts supported on Al-MCM-41 in the catalytic combustion of methane. Particularly, the effect of the preparation procedure and the Pd precursor on the textural, structural and catalytic properties of Pd/Al-MCM-41 materials was studied. Two different preparation methods namely hydrothermal (DHT) and ion-exchange (TIE) using different palladium precursors $Pd(NH_3)_4Cl_2$, $PdCl_2(MeCN)_2$ and $Pd(acac)_2$ were evaluated.

EXPERIMENTAL

1. Chemicals

Cetyltrimethylammonium p-toluenesulfonate, (CTATos; > 99% Merck), Ludox HS-40 (40% SiO_2, Aldrich), sodium hydroxide (Acros), aluminum sulfate–octadecahydrate (98%, Aldrich), tetraammine palladium (II) chloride (99.9%, Alfa Aesar), Palladium (II) acetylacetonate ($Pd(acac)_2$) (34%, ACROS), (acetonitrile) dichloropalladium (II) (99% Accros), ethanol (96%, Elvetec). The sodium silicate solution was prepared as follows: Ludox HS-40 (187 ml) was added to sodium hydroxide (32 g) in deionized water (800 ml) and stirred at 40°C until clear.

2. Synthesis of Al-MCM-41

The catalysts support Al-MCM-41 was prepared by a sol-gel method and using micelles of self-assembled surfactant acting as structuring agents. Al-MCM-41 support was prepared according to the procedure reported in our previous work [28].

A sodium silicate solution (80 ml) was stirred at 60°C for 1 h. A second solution of hexadecyltri-methylammonium p-toluenesulfonate (CTATos, 3.53 g) in deionized water (115 ml) was stirred for 30 min at 60°C. Aluminum sulfate-octadecahydrate ($(Al_2(SO_4)_3.18H_2O)$, 3.53 g) was then added to the latter solution and stirred for 1 h at 60°C. The first solution was added dropwise to the second one, and then stirred at 60°C for 2 h. The obtained gel was transferred in autoclave and heated at 130°C for 20 h. After filtration and washing with deioni-zed water (about 150 ml), the as-synthesized solid was dried at 80°C. The Si/Al ratio in the synthesis gel was equal to 12.5.

3. Catalysts preparation

Pd/Al-MCM-41 catalysts, with nominal Pd loading 1wt% were prepared by using two different routes, namely hydrothermal method and template ion exchange method from different precursors.

a) Hydrothermal method (DHT)

The preparation of catalysts according to the DHT method is a modified synthesis of that adopted by Krawiec et al. [30]. An appropriate amount of Pd $(acac)_2$ dissolved in toluene was added to the solution of surfactant during the preparation of the support. The aluminum precursor was added to the solution containing surfactant similarly to that of the preparation of Al-MCM-41 support. The obtained gel was filtrated through a Buchner funnel, washed with distilled water and then dried at 80°C overnight.

The materials calcined in pure dioxygen at a flow rate of 30 cm^3/min and a temperature ramp of 1°C/min up to a plateau of 550°C for a duration of 7 hours yielded solids ACA-DHT. Indeed, heat treatment allows removing CTA^+ molecules and forming PdO nanoparticles.

b) Template ion-exchange (TIE) method

The preparation of catalysts by TIE method has been reported previously [28]. The support (3.00 g) was added into an aqueous solution (150 mL) of tetraammine palladium (II) chloride, $[Pd(NH_3)_4]Cl_2$ or acetonitrile dichloropalladium(II), $(PdCl_2(MeCN)_2)$. The mixture was vigorously stirred at 80°C for 1 h. After filtration, washing with water (3 x 50 mL) and drying under vacuum at 40°C for 24 h, the resulting solids were calcined similarly to ACA-DHT yielding materials TAM-TIE and ACN-TIE from $Pd(NH_3)_4Cl_2$ and $(PdCl_2(MeCN)_2)$ precursors respectively.

4. Catalyst characterization

• *X-ray diffraction*

XRD patterns were recorded from an automatic diffractometer (Philips Panalytical) using the Cu Kα radiation (λ = 1.5406 Å) and a nickel monochromator. The 2θ range 1- 60° was scanned with a 0.02° step width and an acquisition time of 10 s per step. The reticular distances were compared to those provided by the Joint Committee on Powder Diffraction Standards.

• *Physisorption of N_2*

Both porosity and surface area were investigated from the nitrogen adsorption/ desorption isotherms measured at −196°C using a Micromeritics ASAP 2020 instrument. The BET specific surface area was calculated from the linear part of the BET plot in the reduced pressure range $0.05 < P/P^o < 0.3$. The average pore diameter was calculated using the Barret–Joyner–Halenda (BJH) model on the desorption branch in the reduced pressure range corresponding to the sharp capillary condensation step typical of mesoporous MCM-41 type of materials.

• *UV-Visible Spectroscopy*

UV-visible spectra were recorded using a lambda54 Perkin Elmer spectrophotometer coupled to an integration sphere of RSA-PE- 20 type working in the range 200-900 nm.

• *Temperature-programmed reduction (TPR)*

TPR analyses were measured using an AutoChem 2920 instrument (Micrometrics). Before measurement, 50 mg of calcined catalysts were placed in a quartz tube and heated at 500°C under an argon stream for 1 h and cooled down to 0°C. Then, TPR was carried out in a stream of 5 vol% H_2 in Ar at a flow rate of 15 mL min^{-1} between 0 and 500°C using a temperature ramp of 10°C min^{-1}. The hydrogen concentration in the effluent was monitored on line using a thermal conductivity detector.

• *H_2 chemisorption*

Before H_2 chemisorption, the catalysts were reduced at 500°C under a flow of 5 vol% H_2 diluted in Ar and evacuated in a flow of He at 400°C for 1 h. Then, the adsorption was performed by pulses of 5 vol% H_2 diluted in argon on the solid maintained at 30°C [20, 21].

• *Elemental analysis*

The chemical composition was determined in a Perkin-Elmer 300DV inductively coupled plasma-atomic emission spectrometer (ICP-AES). A standard ICP torch and peristaltic pump was used for all measurements and the accuracy was ranging from 2 to 5%.

5. Catalytic reaction

The methane oxidation tests were performed on a fixed bed catalyst (50 mg, calcined) using a U-shape microreactor. The gas feed mixture (1 vol% CH_4 and 4 vol% O_2 in helium) was flown at a rate of 100 ml min^{-1}. The effluent was analyzed on line using a gas chromatograph equipped with a thermal conductivity detector (TCD) and a Porapak column. The catalysts were all equilibrated in stream of reactant gas for 3 h at 500°C before starting the light-off experiments that were performed by decreasing the temperature of the catalytic bed. A 3 h equilibration at each temperature was applied before measuring the catalytic activity to afford an equilibrated state of the catalysts: a second measurement after waiting for another 3 h gave within the accuracy the same results and allowed to recover similar activities for both preceding and following points. The methane conversion (%) was calculated from the following equations:

$$C_{CH_4} = 100.\left(\frac{X_{CO_2}}{X_{CO_2} + X_{CH_4}}\right)$$

where X_{CO_2} and X_{CH_4} are the molar fraction of the corresponding gas in the feed ($X_i = \frac{P_i}{P_o}$

where P_o is the pressure of the gas at the detector exit, i.e., P_o = 1 atm).

RESULTS AND DISCUSSION

1. Characterization of catalysts

The low angle X-ray diffraction (XRD) patterns of the materials showed an ordered hexagonal

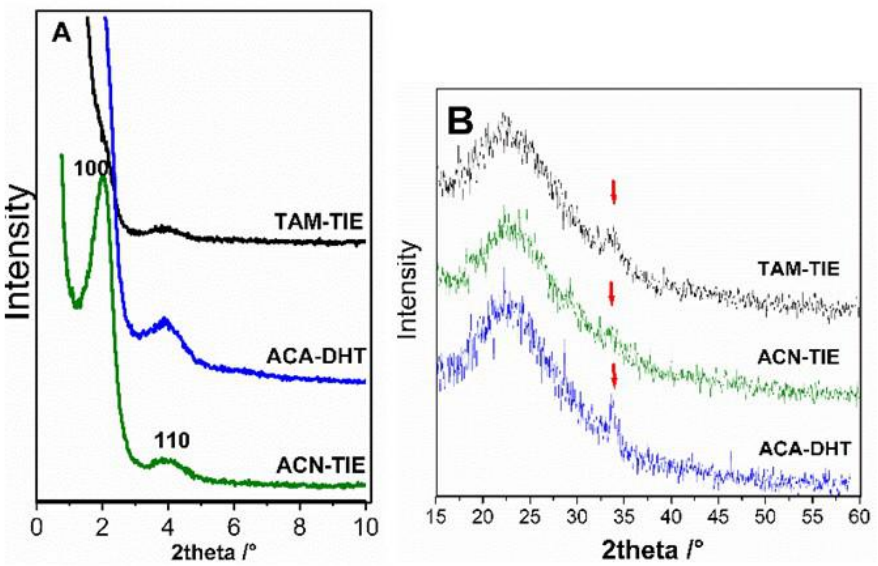

Figure 1: XRD patterns of TAM-TIE, ACN-TIE and ACA-DHT catalysts at low diffraction angles (A) and at high diffraction angles (B).

mesostructure (Figure 1A). Indeed, the intensities and positions of the peaks assigned to the reflections (100) and (110) confirm the 2D hexagonal arrangement of the pores for ACN-TIE and ACA-DHT catalyst. However, the absence of a well-defined (100) reflection for TAM-TIE sample showed a significant collapse of the pore structure At higher angles, the narrow peak appearing at 2θ = 33° is assigned to the (101) reflection of the PdO phase [31-32], while the broader one at 24° is a scattering peak typical of amorphous silica [28] (Figure 1B). The Absence of the characteristic peaks of PdO at 2θ = 41.9° ; 54.5° ; 60.2° ; 60.7° et 71.3° confirms that these nanoparticles are more dispersed than those in the PdO/MCM-41(0.5) catalyst prepared by Hernández-Pineda et al. [32]. The results show that the use of different palladium precursors affects the crystalline structure of obtained materials, and that the intensity of the peak characteristic of the PdO phase (2θ = 33°) decreases according to this order: ACN-TIE > TAM-TIE > ACA-DHT. It is also noted that the catalysts prepared by hydrothermal method have the smallest PdO particles.

The nitrogen adsorption– desorption isotherms at 77 K of ACN-TIE, TAM-TIE and ACA-DHT are shown in Figure 2. It can be seen clearly that the obtained isotherms of the samples can be classified as type IV indicating the presence of uniform mesopores [12].

A comparison of the isotherms indicates that those relating to the catalysts prepared with the same method are superposable with a shift towards higher volumes of adsorbed N_2 for the catalyst prepared by the TIE method.

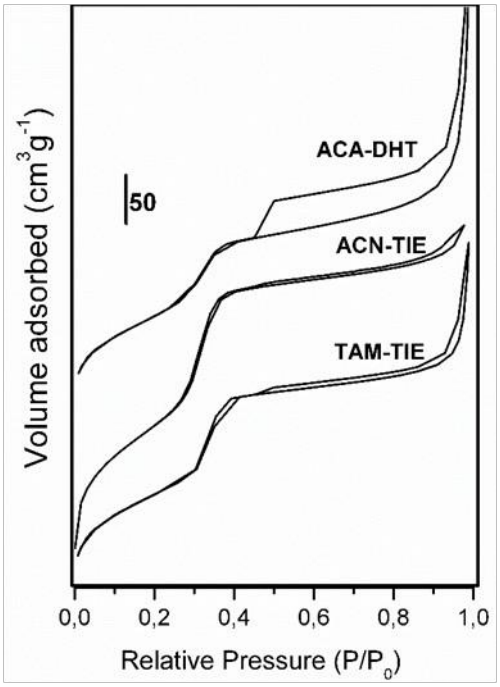

Figure 2: N_2 adsorption-desorption isotherms of TAM-TIE, ACN-TIE and ACA-DHT samples at 77 K.

Table I. Specific BET surface areas, pore volume and mean pore diameter of TAM-TIE, ACN-TIE and ACA-DHT catalysts.

Catalyst	BET area (m^2/g)	Pore volume (cm^3/g)	mean pore diameter (nm)
TAM-TIE	470	0.46	3.40
ACN-TIE	727	0.70	3.29
ACA-DHT	519	0.50	3.96

Moreover, It can be seen that both TAM-TIE and ACN-TIE samples exhibit type-IV isotherms with H1 hysteresis loop similar to the ACA-DHT catalyst with a widening of the hysteresis loop. This, suggests that for the latter, the porous distribution is less homogeneous by having a wider pore diameter (Table I). Consequently, it is found that the surface area and the pore volume of the TAM-TIE catalyst are lower than those of ACA-DHT and ACN-TIE. The use of acetonitrile dichloropalladium(II) as precursor by the TIE method generated a BET surface area of 727 m²/g (Table I) , higher than that of TAM-TIE catalyst of 275 m²/g. The reason for such a loss of pore volume Vp for TAM-TIE and ACA-DHT catalysts is due, for one part, to channel plugging by the presence of PdO particles and, for the other part, to the partial collapse of the TAM-TIE support structure. This has led to the closure of nano-channels, which is probably due to the dominant effect according to the XRD results.

The UV-visible diffuse reflectance was performed to study the nature of palladium particles in the catalysts. The spectra of the catalysts (Figure 3) were similar and composed of superposed broad bands not fully resolved the intensities of which varied with the type of the palladium precursor, as well as the method of preparation. The main bands arose at ca. 210 nm (small), 320 nm (medium, shoulder), 350 - 400 nm (strong and structured) and 460 nm (strong). Despite some ambiguities in assessing the intensities of broad band and band overlap in the spectral range 300 - 600 nm, it appears that all bands follow the same trend. The bands ranging in between 200 and 380 nm are usually assigned to metal-ligand charge transfer transitions between Pd^{2+} and O^{2-} ions of PdO particles [33]. However, the broad absorption band at 460 nm is rather assigned to d–d electronic transitions of Pd^{2+} ions [34], this band appears more intense for ACA-DHT sample. Moreover, taking into account of the assumption of Cónsul et al.[35] who have admitted that the relative intensities of the d-d bands depends on particle size, we can confirm the presence of a larger PdO nanoparticles for ACA-DHT. This result assumes a lower metal dispersion of the latter than those prepared by the ion-exchange method.

The variation in the intensity of this band indicates that Pd^{2+}, other than those of the PdO clusters are present and should be also related to weak field ligands , likely those of the support such, i.e., silanol, silanolate, siloxane or aluminosiloxane surface groups (SiOH, SiO^-, Si-O-Si, Si-O-Al

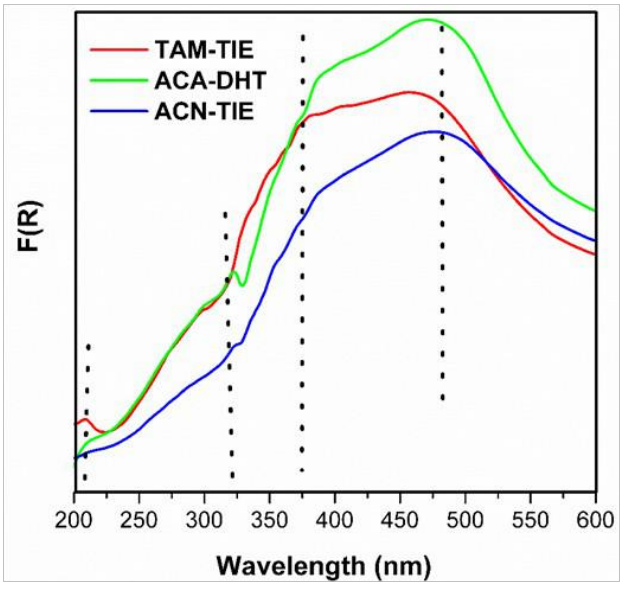

Figure 3 : Diffuse reflectance UV–vis spectra of TAM-TIE, ACN-TIE and ACA-DHT catalysts.

Table II. The metallic dispersion of Pd is measured by hydrogen chemisorption and size of Pd nanoparticles in solid samples estimated from Scherrer's equation.of TAM-TIE, ACN-TIE and ACA-DHT catalysts.

Catalyst	$PdO_{(DRX)}$ particle size (nm)	Pd (%wt)	H/Pd(%)	Conversion (%) at 500°C	T_{50} (°C)
TAM-TIE	23	0.97	4	80	416
ACN-TIE	38	1.00	14	93	385
ACA-DHT	15	1.00	1.6	35	> 500

respectively). These ions are probably oligomeric Pd^{n+} species where n = 1, 2 or 3, which are known to act as "chemical glue" [36, 37]. An inverse tendency of the intensities of UV spectra bands relative to metal dispersion has been reported. This indicates that the formation of Pd^{n+} ions is not necessary to promote high dispersion more likely depending on the preparation method and on the eventual presence of Al in the support [35].

The palladium dispersion was explored by applying the Scherrer equation to the XRD line broadening assigned to the "XRD detectable" PdO phase (Figures 1B, Table II) [38]. This method allowed to calculate the average PdO particle sizes of 23 ; 38, and 15 nm for TAM-TIE, ACN-TIE et ACA-DHT, respectively. According to XRD results, it has be shown that PdO nanoparticles size in catalysts prepared by the hydrothermal method (DHT) are smaller than those prepared by the ion exchange method (TIE), this seems consistent with highly dispersed Pd nanoparticles in ACA-DHT catalyst.

Further evaluation of the metal dispersion using hydrogen chemisorption was necessary and results are provided in table II. These data clearly showed a low metal dispersion despite an increasing content of palladiumfor the catalyst prepared by DHT method. This is in contradiction with XRD data showing smaller particles sizes and also with the expected effect of Al reported by Yoshida et al. [27]. Since, hydrogen chemisorption analysis is limited to the external surface of the support, we can conclude that a high proportion of PdO nanoparticles are well dispersed along the inner surface of channel wall.

Therefore, these results suggest that PdO nanoparticles are mainly located inside the framework of MCM-41 for DHT samples, which make them inaccessible to hydrogen. On the other hand, with the TIE method, a highly dispersed metal particles (H/Pd(%) = 14) were obtained by using palladium $PdCl_2(MeCN)_2$ precursors as compared to the $Pd(NH_3)_4Cl_2$ precursor. Which is in contradiction with the XRD results, highly dispersed metal particles were obtained on TAM-TIE catalysts. It is considered coherent to think that PdO particles on TAM-TIE catalysts were rendered inaccessible to hydrogen because of channel closure and structure (Figure 1A) collapse onto the particles.

On the other hand, positive peaks between 50° and 80°C. due to the desorption of hydrogen are due to the decomposition of the PdH_2 hydride formed during the passage of H_2 at low temperature and the recapture of d In the circuit.

Temperature-programmed reduction of the catalysts characterizes the temperatures at which the PdO phase starts to be reduced with the appearance of a negative peak corresponding to

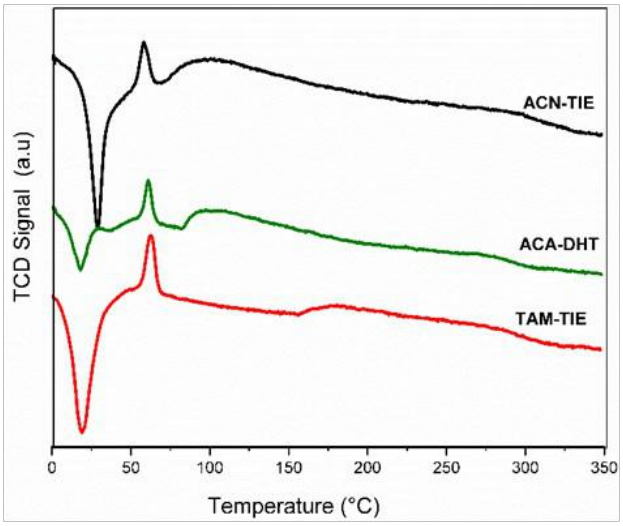

Figure 4 : H_2-TPR curves of the composite catalysts.

hydrogen consumption (Figure 4). On the other hand, positive peak appeared in the range of 50 - 80°C due to the desorption of hydrogen is attributed to the decomposition of PdH_2 hydride phase which occurs at low temperature and recapture of hydrogen in the circuit [39] (Figure 4). A sharp positive and intense peak, confirm that the formation of the metallic phase below this temperature, since the Pd particles are reduced at lower temperatures. However, desorption of hydrogen at a temperature above 80°C, characterized by the presence of long tails up to 250°C, can be assigned to NiO particles weakly bound to the Al-MCM-41 support and also those already reduced below 0°C [40]. The reduction peak relative to the ACN-TIE catalyst (at 28°C) is 10°C higher than that of the TAM-TIE catalyst (at 18°C), suggesting a stronger interaction between palladium oxide and the support for the catalyst prepared from the $PdCl_2(MeCN)_2$ precursor.

The TIE method provides more reducible particles than those formed by hydrothermal (DHT) method. Moreover, a decrease in the width of the reduction peak is observed, indicating that the palladium species are more homogeneous and better dispersed. Indeed, this result is in agreement with H_2 chemisorption measurements, where a dispersion of 14 and 4% were recorded for ACN-TIE and TAM-TIE, respectively.

The results obtained are consistent with the literature, which shows that the nature of palladium precursors and the method of preparation considerably affect the reducibility and the metallic dispersion of PdO species [29]. However, the template ion-exchange (TIE) method by using (acetonitrile) dichloropalladium(II) as the palladium precursor generated highest PdO particles dispersion.

2. Methane oxidation catalytic test

In this work, we have followed the catalytic activity of the elaborated mesoporous materials in the catalytic combustion of methane as a function of time and temperature. The catalysts were rather stable under reaction conditions yielding only CO_2 and H_2O consistent with a complete oxidation of methane.

The effect of Pd precursor has been studied by determining the activity of the ACN-TIE, TAM-TIE and ACA-DHT catalysts, in the isothermal regime for 3 h at 500°C (Figure 5-A). The results showed that palladium-based catalysts supported on Al-MCM-41 and prepared by the TIE method are the most active and have profiles beginning of activity as a function of time almost similar.

The evolution of methane conversion over time for all catalysts shows that the activity rose slightly and do not reach the steady state even after 3 hours of reaction unlike the palladium-based catalysts deposited on the Y zeolite which stabilize at 500°C after about 30 min of reaction [11]. The conversion of the methane determined after 3 h of reaction at 500°C shows that the conversion rate increases in the following order: ACN-TIE > TAM-TIE > ACA-DHT. Moreover, the activities for all the catalysts increase linearly after 1 h of reaction, with a parallel variation for TAM-TIE and ACA-DHT catalysts. Indeed, at t > 1h the variation of the conversion d[A]/dt is 0.11 for ACN-TIE and 0.06 for TAM-TIE et ACA-DHT catalysts.

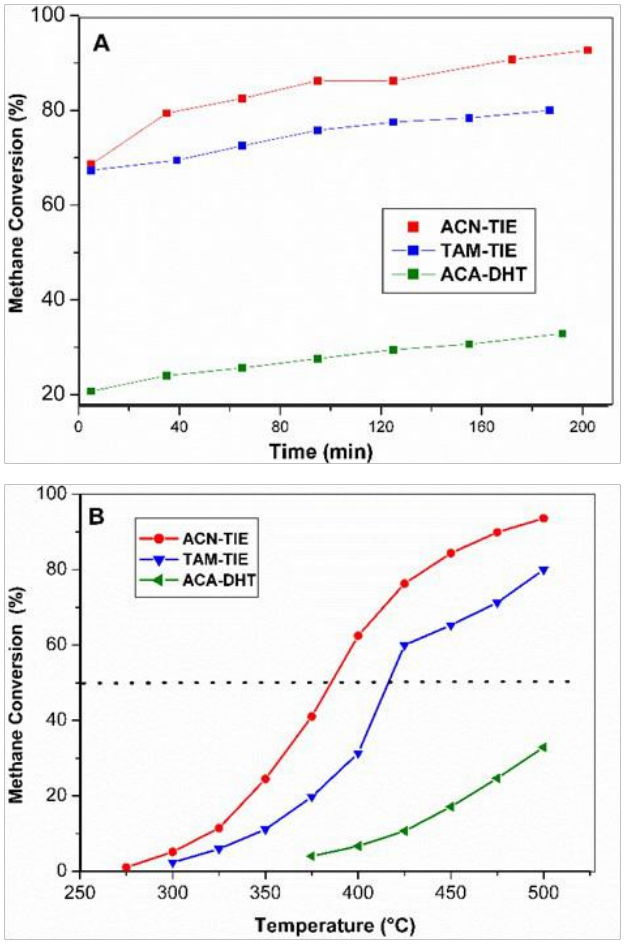

Figure 5 : Methane conversion as function of (A) reaction time and (B) reaction temperature for TAM-TIE, ACN-TIE and ACA-DHT catalysts.

The results show (figure 5A) that the ACN-TIE sample exhibited around 80% CH_4 conversion after 35 min of reaction, whereas for the TAM-TIE catalyst, this conversion rate was achieved only after 188 min. Indeed, taking into account the variation d[A]/dt, we can simulate the reaction time of about 20 h in order to achieve 100% conversion for the most active catalyst (ACN-TIE). The above results clearly show that methane oxidation conversion is strongly influenced by the nature of metal precursor and the method of catalysts preparation. In fact, the $PdCl_2(MeCN)_2$ precursor and the ion exchange method are the most appropriate to promote the catalytic activity of the palladium in the methane combustion.

In the following, we have studied the evolution of the methane conversion as a function of the reaction temperature ranging from 250° up to 500°C for ACN-TIE, TAM-TIE and ACA-DHT catalysts (Figure 5-B). The light-off methane combustion curves show that over the entire temperature range studied, the ACN-TIE catalyst exhibits the highest catalytic activity. It can be also clearly seen that all samples are relatively inactive at temperatures below 250°C. The evaluation of the temperatures T_{50} corresponding to the methane conversion rate of 50%, shows that the ACN-TIE sample having the lowest T_{50} (38°C) is the most active (Table II).

Elemental Analysis of materials by ICP measurements (Table II) had revealed for all samples similar Pd contents of ca. 1 wt%. However the results show that the ACN-TIE sample exhibited the highest catalytic activity. This result can be correlated with the textural characteristics (S_{BET} and V_p) of the latter sample and more probably with the highest dispersion of the PdO nanoparticles for the catalyst prepared from $PdCl_2(MeCN)_2$ precursor, compared to that prepared from $Pd(NH_3)_4Cl_2$, which is in agreement with the results described in literature [22]. Moreover, the PdO nanoparticles in the TAM-TIE catalyst are characterized by a low interaction with the Al-MCM-41 support compared to the ACN-TIE catalyst, proving that the decrease of catalytic activity for TAM-TIE catalyst is strongly correlated with the low reducibility of the PdO nanoparticles. However, the results show that the ACA-DHT catalyst is the worst performing although it has the smallest PdO particles as well as a reduction temperature (18°C) comparable to that obtained for the TAM-TIE catalyst (19°C). The latter showed a better dispersion of the active phase as well as a better catalytic activity compared to the ACA-DHT material. According to the obtained results our study confirms that the metal dispersion is one factor that affects much more the catalytic performances rather than the metal reducibility. It appears that palladium is less accessible to methane when the catalyst is prepared by the DHT method, which explains the differences in catalytic activity of Pd in methane combustion amongst the two synthesis methods TIE and DHT.

CONCLUSION

A series of palladium catalysts supported on aluminosilicate mesoporous silica Al-MCM-41 characterized by a 2D hexagonal lattice were prepared according to direct hydrothermal (DHT) and template ion exchange (TIE) methods, which led to different catalytic properties.

In fact, template ion-exchange method, generate a good catalytic activity for ACN-TIE sample were prepared by $PdCl_2(MeCN)_2$ precursor. Modification of palladium dispersion and the reducibility associated with depending on the precursor used, resulting in different catalytic properties toward methane combustion. Furthermore, the data indicates that, in the conditions employed in this work, the template ion-exchange method and $PdCl_2(MeCN)_2$ are a suitable precursor for preparing Pd/Al-MCM-41 catalysts as the most active in the total combustion of methane. It appears that palladium is less accessible to methane when the catalyst is prepared by the DHT method, which explains the differences in catalytic activity of Pd for the combustion of methane between the two catalysts synthesized by the TIE and DHT methods.

REFERENCES

[1] D. Cheng, K. Okumura, Y. Xie, C.-J. Liu, Appl. Surf. Sci., **2007**, 254, 1506.
[2] B. Yue, R. Zhou, Y. Wang, X. Zheng, Appl. Surf. Sci., **2006**, 252, 5820.
[3] K. Persson, L.D. Pfrefferle, W. Schwartz, A. Ersson, S.G. Järås, Appl. Catal. B, **2007**,74, 242.
[4] R.J. Farrauto, Science, **2012**, 337, 659.
[5] P. Gélin, M. Primet, Appl. Catal. B, **2002**, 39, 1.
[6] J.R. Paredes, E. Díaz, F.V. Díez, S. Ordónez, Energy Fuels, **2009**, 93, 2386.
[7] S. Zribi, B. Albela, L. Bonneviot, M. Saïd Zina, Appl. Catal. A, **2015**, 502, 195.
[8] F. Yin, S. Ji, P. Wu, F. Zhao, C. Li, J. Catal, **2008**,

257, 108.
[9] J.-H. Park, B. Kim, C.-H. Shin, G. Seo, S.H. Kim, S.B. Hong, Top. Catal., **2009,**52, 27.
[10] S. Zribi, M. Saïd Zina, Reac. Kinet. Mech. Cat., **2016**, 118, 577.
[11] H. Najar, M.S. Zina, A. Ghorbel, Kinet. Kata., **2010**, 51, 602.
[12] G. Groppi, C. Cristiani, L. Lietti, C. Ramella, M. Valentini, P. Forzatti, Catal. Today, **1999**, 50, 399.
[13] K. Okumura, S. Matsumoto, N. Nishiaki, M. Niwa, Appl. Catal. B, **2003**, 40, 151.
[14] H. Maeda, Y. Kinoshita, K.R. Reddy, K. Muto, S. Komai, N. Katada, M. Niwa, Appl. Catal. A, **1997,** 163, 59.
[15] K. Okumura, E. Shinohara, M. Niwa, Catal. Today, **2006**, 117, 577.
[16] J.A.C. Ruiz, M. A.Fraga, H. O.Pastore, Appl. Catal. B, **2007**, 76, 115.
[17] Z.J. Wang, Y. Liu, P. Shi, C.J. Liu, Y. Liu, Appl. Catal. B, **2009**, 90, 570.
[18] J. Bassil, A. AlBarazi, P. D.Costa, M. Boutros, Catal. Today, **2011**, 176, 36.
[19] N. Krishnankutty, J. Li, M.A. Vannice, Appl. Catal. A, **1998**, 173, 137.
[20] K. Fujimoto, F.H. Ribeiro, M. Avalos-Borja, E. Iglesia, J. Catal., **1998**, 179, 431.
[21] J.A.C. Ruiz, E. C. Oliveira, M.A. Fraga, H. O. Pastore, Catal. Commun., **2012,** 25, 1.
[22] P. Castellazzi, G. Groppi, P. Forzatti, A. Baylet, P. Marecot, D. Duprez, Catal. Today, **2010**,155, 18.
[23] P. Castellazzi, G. Groppi, P. Forzatti, E. Finocchio, G. Busca, J. Catal., **2010**, 275, 218.
[24] B.H. Yue, R.X. Zhou, Y.J. Wang, X.M. Zheng, J. Mol. Catal. A 238, **2005**, 238, 241.
[25] M.A. Fraga, E.S. de Souza, F. Villain, L.G. Appel, Appl. Catal. A: Gen, **2004**, 259, 57.
[26] T.V. Choudhary, S. Banerjee, V.R. Choudhary, Appl. Catal. A, **2002**, 234, 1.
[27] H. Yoshida, T. Nakajima, Y. Yazawa, T. Hattori, Appl. Catal. B, **2007,** 71, 70.
[28] A. Gannouni, B. Albela, M. Saïd Zina, L. Bonneviot, Appl. Catal. A, **2013**, 116, 464.
[29] L.M.T. Simplicio, S.T. Brandao, E.A. Sales, L. Lietti, F. Bozon-Verduraz, Appl. Catal. B, **2006**, 63, 9.
[30] P. Krawiec, E. Kockrick, P. Simon, G. Auffermann, S. Kaskel, Chem. Mater., **2006**, 18, 2663.
[31] T. Kawabata, I. Atake, Y. Ohishi, T. Shishido, Y. Tian, K. Takaki, K. Takehira, Appl. Catal. B, **2006**, 66, 151.
[32] J. Hernández-Pineda, J.M. del Río, E. Carreto, E. Terrés, J.A. Montoya, M.J. Zuñiga-González, J. Morgado, J. Alloys Compd., **2009**, 481, 526.
[33] E. D. Garbowski, J. Phys. Chem., **1978**, 75, 226.
[34] A.N. Pestryakov, V.V. Lunin, S. Fuentes, N. Bogdanchikova, A. Barrera, Chem. Phy. Lett., **2003**, 367, 102.
[35] J.M.D. Cónsul, C.A. Peralta, E.V. Benvenutti, J.A.C. Ruiz, H.O. Pastore, I.M. Baibich, J. Mol. Catal. A, **2006,** 246, 33.
[36] M. Tzou, H. Jiang, W. Sachtler, Appl. Catal.,**1986**, 20, 231.
[37] A. Gannouni, X. Rozanska, B. Albela, M. Saïd Zina, F. Delbecq, L. Bonneviot, A. Ghorbel, J. Catal., **2012**, 289, 227.
[38] O. Mekasuwandumrong, S. Somboonthanakij, P. Praserthdam, J. Panpranot, Ind. Eng. Chem. Res., **2009**, 48, 2819.
[39] P. Sangeetha, K. Shanthi, K.S. Rama Rao, B. Viswanathan, P. Selvam, Appl. Catal. A: Gen, **2009**, 353, 160.
[40] M.L. Cubeiro, J.L.G. Fierro, Appl. Catal. A: Gen, **1998**, 168, 307.